Computers, Environment and Urban Systems xxx (xxxx) xxx–xxx

Contents lists available at ScienceDirect

Computers, Environment and Urban Systems

journal homepage: www.elsevier.com/locate/ceus

A GIS tool for cost-effective delineation of flood-prone areas

Caterina Samela, Raffaele Albano, Aurelia Sole, Salvatore Manfreda*

Università degli Studi della Basilicata, Potenza 85100, Italy

ARTICLE INFO

Keywords:
Flood susceptibility
Digital Elevation Model (DEM)
Geomorphic Flood Index
Linear binary classification
Data scarce environments
Geographic Information System (GIS)

ABSTRACT

Delineation of flood hazard and flood risk areas is a critical issue, but practical difficulties regularly make complete achievement of the task a challenge. In data-scarce environments (e.g. ungauged basins, large-scale analyses), useful information about flood hazard exposure can be obtained using geomorphic methods. In order to advance this field of research, we implemented in the QGIS environment an automated DEM-based procedure that exhibited high accuracy and reliability in identifying the flood-prone areas in several test sites located in Europe, the United States and Africa. This tool, named Geomorphic Flood Area tool (GFA tool), enables rapid and cost-effective flood mapping by performing a linear binary classification based on the recently proposed Geomorphic Flood Index (GFI). The GFA tool provides a user-friendly strategy to map flood exposure over large areas. A demonstrative application of the GFA tool is presented in which a detailed flood map was derived for Romania.

1. Introduction

Floods are the most frequently occurring and costliest natural hazard throughout the world, and flood damages constitute about a third of the economic losses inflicted by natural hazards (Munich, 2005). In the period 1975–2001, a total of 1816 flood events killed over 175,000 people and affected > 2.2 billion worldwide (Jonkman, 2005). Moreover, the United Nations (UNISDR and CRED, 2015) has estimated that one third of the world's population (around 2.3 billion people) has been effected by flood in the last 20 years.

Flood inundation maps are at the base of flood risk management, informing the public and city planners about flood-prone areas in a region. Most flood inundation maps are developed by computer modelling, involving hydrologic analyses to estimate the peak flow discharge for assigned return periods, hydraulic simulations to estimate water surface elevations, and terrain analysis to estimate the inundation area (Alfieri et al., 2014; Bradley, Cooper, Potter, & Price, 1996; Knebl, Yang, Hutchison, & Maidment, 2005; Sole et al., 2013; Whiteaker, Robayo, Maidment, & Obenour, 2006).

Despite recent advancements in computational techniques and availability of high-resolution topographic data, flood hazard maps are still lacking in many countries. The main difficulty in using a specific method or model is primarily correlated to the significant amount of data and parameters required by these models. Thus, their calibration and validation is a rather challenging task, especially considering that gauging stations are heterogeneously and unevenly distributed (Di Baldassarre, Schumann, & Bates, 2009). This is especially relevant in developing countries, which suffer from weak coping strategies and inefficient mechanisms for disaster management due to limited resources for flood protection. Traditional modelling approaches are costly, making them unaffordable not only for developing countries, but also for more developed ones. For instance, in the U.S., many rural counties and several minor tributaries do not have any associated flood inundation information. FEMA (Federal Emergency Management Agency) (2006) estimated that flood inundation mapping could cost from $3000 to $6000/km of river reach in the U.S. Therefore, there is a need to look for efficient and inexpensive ways to derive flood inundation maps.

In this scenario, several studies have demonstrated that flood-prone areas can be delineated using methods which rely on geomorphologic characterization of a river basin (Clubb et al., 2017; De Risi, Jalayer, & De Paola, 2015; Degiorgis et al., 2012; Dodov & Foufoula-Georgiou, 2006; Gallant & Dowling, 2003; Jafarzadegan & Merwade, 2017; McGlynn & Seibert, 2003; Nardi, Vivoni, & Grimaldi, 2006; Noman, Nelson, & Zundel, 2001; Wolman, 1971). A mutual causal relationship exists between flooding and the shape and extension of floodplains, since fluvial geomorphology is essentially shaped by flood-driven phenomena (Arnaud-Fassetta et al., 2009; Nardi, Biscarini, Di Francesco, Manciola, & Ubertini, 2013).

Given this assumption, we have developed a practical and cost-effective procedure (proposed by Samela, Troy, & Manfreda, 2017) to preliminarily delineate flood-prone areas in poor data environments and for large-scale analyses based on easily available information.

* Corresponding author.
E-mail address: salvatore.manfreda@unibas.it (S. Manfreda).

https://doi.org/10.1016/j.compenvurbsys.2018.01.013
Received 29 July 2017; Received in revised form 29 January 2018; Accepted 30 January 2018

2. Background of the project

The above-mentioned research stems from an idea proposed by Manfreda, Di Leo, and Sole (2011) of using a topographic descriptor of the surface in order to obtain preliminary indications about the flood exposure of a basin. The authors suggested using a modified version of the Topographic Index (*TI*) developed by Beven and Kirkby (1979) to detect flood hazard exposure. The authors compared the modified *TI* and flood inundation maps obtained from hydraulic simulations and observed that the portion of a basin exposed to flood inundation is generally characterized by a TI_m higher than a given threshold, τ. Therefore, they proposed a GRASS GIS tool (Di Leo, Manfreda, & Fiorentino, 2011) that adopts the TI_m to delineate the flood prone areas using simple regression functions to estimate the parameters τ and n. Interestingly, they observed that both parameters are strongly controlled by the cell size of the Digital Elevation Model (DEM).

Later on, Manfreda, Nardi, et al. (2014) carried out a comparative analysis between three different geomorphic procedures: the modified *TI* by Manfreda et al. (2011), the linear binary classifiers method by Degiorgis et al. (2012, 2013) and a hydrogeomorphic algorithm by Nardi et al. (2013, 2006) over the Upper Tiber River and Chiascio River basin. This study proved that a preliminary delineation of the flood-prone areas can be carried out using procedures that rely on basin geomorphologic features, and provided an initial investigation about the role played by some morphologic features on flood exposure. Analysing performances, flexibility, and structure complexity, the linear binary classification has proven to be the most appealing tool since it showed good detection performance with simple requirements in terms of input data, costs, and computational times. It allows implementation of a binary classification based on any morphologic descriptor or combination of descriptors and derivation of a flood susceptibility map over large areas starting from the study of a small portion of the basin; it also requires the calibration of a single parameter.

Motivated by these observations, several studies have been dedicated to understanding which geomorphic attributes are the most predictive with regard to the flood inundation process, and how to use these descriptors to map the flood exposure over large spatial scales. To this purpose, eleven morphological descriptors presumed to be good candidates as indicators of flood hazard exposure were tested to identify the performances in different hydrologic, climatic and topographic contexts: in several Italian gauged basins; an ungauged basin in Africa (Bulbula River, Ethiopia) (Manfreda, Nardi, et al., 2014; Manfreda et al., 2015; Manfreda, Samela, et al., 2014; Samela et al., 2016); and over the entire continental U.S., moving from basin-scale analyses to a continental-scale application (Samela, Manfreda, & Troy, 2017; Samela, Troy, et al., 2017).

In light of this extensive investigation, the classifier based on the Geomorphic Flood Index (GFI) consistently exhibited higher classification accuracies compared to the others in each test. Moreover, it presented a low sensitivity to changes in the input data in terms of dominant topography of the training area, size of the training area, DEM resolution, standard flood maps adopted (1-D or 2-D hydraulic model), return time, and scale of the analysis (Samela, Troy, et al., 2017). Therefore, GFI has been acknowledged as the most suitable morphologic classifier among those examined for preliminary mapping over large unstudied areas and in data-sparse environments.

With the specific aim of transferring the knowledge acquired from these years of research to the scientific and technical community, the full procedure has been implemented in a new plugin named Geomorphic Flood Area tool (GFA tool), working in the open-source Geographic Information System Quantum GIS (QGIS). In fact, the transfer of scientific findings from the research to a wider range of users is an important component of progress for the society that may benefit from an advance in flood mapping techniques. The tool has a user-friendly interface and enables rapid detection of flood-prone areas starting from readily available data. It also allows generation of complementary information like the GFI, which may be used as river basin descriptor in other applications such as detection of inundated areas by remote sensing techniques (e.g. D'Addabbo et al., 2016) and delineation of floodplains.

The GFA tool source code is published under free and open-source software licenses with end-user rights to analyse, modify and redistribute it for any purpose. Anyone can contribute to the methodologies/algorithms adopted and further develop and exploit the technology into new products, processes, applications, materials, or services generating new data through a community-based development process.

3. The Geomorphic Flood Area tool

3.1. Method description

The Geomorphic Flood Area tool makes it possible to derive a flood susceptibility map of a basin by combining geomorphological information extracted by DEMs along with flood hazard information from existing inundation maps which are usually available for limited portions of a basin. This is achieved by classifying the points within a basin into two groups – flood-prone areas and areas not prone to floods – by using a linear binary classifier based on the Geomorphic Flood Index (GFI) (Samela, Troy, et al., 2017). The index has been defined as:

$$\ln\left(\frac{h_r}{H}\right) \tag{1}$$

It compares in each point of the basin the water level h_r in the nearest element of the river network identified following the hydrological paths ('r' stands for 'river'), with the elevation difference (H) between these two points. h_r is estimated as a function of the contributing area using the hydraulic scaling function proposed by Leopold and Maddock (1953) and more recently investigated by Nardi et al. (2006) (see Eq. (2)):

$$h_r \approx A_r^n \tag{2}$$

where h_r is the water depth [m], A_r [km^2] is the contributing area calculated in the nearest point of the river network hydrologically connected to the point under examination, and n is the exponent (dimensionless).

The relationship between the GFI and the standard flood map, and therefore the linear boundary of decision between the two classes, is first calibrated within a training area, and then applied to map the flood susceptible areas at the basin scale. This boundary is expressed by a value of a threshold and, according to the analyses of Samela, Troy, et al. (2017), a calibration area equal or larger than 2% of the basin of interest is required in order to calibrate the optimal threshold.

This method can be useful when there is an absence of detailed data for flood simulations and provides preliminary indications about locations geomorphologically prone to floods. The analysis can be performed using data freely available online (nowadays several free DEM sources exist, especially for research purposes), and is therefore economic and fast. The method works consistently over a range of dominant topographies, available calibration areas (minimum required is 2% of the basin of interest), spatial scales, and DEM resolutions (Samela, Troy, et al., 2017).

However, this kind of analysis does not consider the physical processes of runoff generation, and cannot describe flood propagation in space and its interaction with infrastructures (e.g. bridges or artificial obstacles). Nevertheless, this preliminary information may be useful to identify the most critical locations and to define the computational domain of a hydraulic model for more detailed studies when needed, as suggested for other DEM-based methods (e.g. Nardi et al., 2006).

We underline that in areas were hydrologic, hydraulic and topographic information can be obtained to perform a proper hydraulic study, that study must be undertaken.

3.1.1. Input data

This geomorphic approach requires two main sets of input data:

i. a Digital Elevation Model (DEM) to calculate the Geomorphic Flood Index;
ii. a detailed flood hazard map usually derived from hydraulic models, representing the reference standard data used to train the linear binary classifier based on the GFI (e.g. maps provided by river basin authorities or emergency management agencies). This calibration map, in the form of a raster grid, is necessary for limited portions of the basin of interest.

Supported raster formats are GeoTiff (*.tiff) and ASCII ESRI GRID format (*.txt or *.asc).

Like almost all applications related to water resources management and hydrological modelling, this procedure benefits from high-quality DEMs since the elevation data is the fundamental input of the tool and its accuracy and resolution influence the reliability of the results. The vertical accuracy of the grid cell elevation is a critical factor as a small error in elevation (e.g. missing data points, voids and unreal sinks) may propagate through model predictions and produce incorrect identification of hydrological features, such as watershed boundaries, and simulated drainage networks that do not correspond to the actual ones. This can result in incorrect values of the spatial variables derived from the DEM and totally different predictions. The grid resolution can also profoundly impact DEM-derived attributes, as noted by several researchers (e.g. Kenward, 2000; Wu, Li, & Huang, 2008). The general rule regarding resolution is to adopt a DEM where generalisations of the land surface are within the spatial range of the processes under investigation, otherwise results must be treated with caution (Vaze, Teng, & Spencer, 2010). In our context, the higher the resolution, the better the flood susceptible areas can be identified (i.e. at a finer scale). Therefore, the best option is adopting DEMs derived from airborne LiDAR (Light Detection and Ranging), which exhibits higher horizontal resolution and vertical accuracy. However, their use is not always feasible and so several on-line DEMs with a horizontal resolution of 30–90 m may be a useful source in data-scarce regions and/or for large-scale studies (Yan, Di Baldassarre, Solomatine, & Schumann, 2015). An evaluation of on-line DEMs for flood inundation modelling was carried out by Sanders (2007) who concluded that the added precision of LiDAR will likely justify the cost in developed countries, but also highlighted the utility of SRTM (Shuttle Radar Topography Mission) as a global source of terrain data for flood modelling in cases where high resolution surveys are cost-prohibitive and there are other larger factors of uncertainty.

With regard to the calibration map, the user can reasonably utilize any flood hazard map available from official sources (e.g. emergency management agencies, river basin authorities, Federal or State agencies, etc.) as possible sources of gold standard flood hazard data. If authoritative flood hazard mapping is not available, historical flood heights or other information can provide guidance. Information from other sources (e.g. maps produced by universities or research centers) should be used as the basis for calibration of the GFI. Obviously, it is likely that this data may contain uncertainties and errors, but it represents the best available data.

3.1.2. Pre-processing

To calculate the GFI, a terrain analysis on the DEM is performed. Standard raster processing for hydrologic applications requires that all cells within the DEM contribute water to an adjacent cell. To assign flow directions to cells, they must have downslope cell neighbours (Schwanghart & Kuhn, 2010).

Nevertheless, DEMs, like other spatial data sets, are subject to errors. They are affected by different kinds of irregularities not always representing natural features, such as sinks (Olivera, Famiglietti, & Asante, 2000), depressions (Lindsay & Creed, 2005; Planchon & Darboux, 2002) and pits (Grimaldi, Nardi, Di Benedetto, Istanbulluoglu, & Bras, 2007; Soille, 2004). These spurious errors may cause flow discontinuities, making it difficult to correctly characterize the flow direction and its derivatives (e.g. Jenson & Domingue, 1988; Lindsay & Creed, 2005; Martz & Garbrecht, 1998; Nardi, Grimaldi, Santini, Petroselli, & Ubertini, 2008; O'Callaghan & Mark, 1984). To improve the performance of a DEM for hydrological applications, adoption of a hydrologically conditioned DEM where the original data have been conditioned and improved to force the DEM to produce correct river network topology (e.g. HydroSHEDS conditioned DEM) is suggested. Alternatively, it is convenient to create a filled DEM, where all cells that contain an elevation value lower than their neighbouring eight cells (sinks) are “filled” to the elevation at which they will outlet water to an adjacent cell of lesser value. This conditioning process, commonly referred to as pit filling, alters the original elevation data so it must be used only for deriving the drainage network and the related variables. It is implemented in most common GIS software, including ESRI ArcGIS, Quantum GIS and GRASS. Since its main drawback is the possible creation of large flat regions, users may decide to implement more detailed treatments during DEM pre-processing to predict more realistic drainage patterns and slopes, and positively influence geomorphic model results (see the works of Garbrecht & Martz, 1997; Grimaldi et al., 2007; Lindsay & Creed, 2005; Martz & Garbrecht, 1999; Nardi et al., 2008; Planchon & Darboux, 2002; Santini, Grimaldi, Nardi, Petroselli, & Rulli, 2009; Soille, 2004; Tianqi, Takeuchi, Ishidaira, Yoshitani, & Fukami, 2003; Wang & Liu, 2006).

A flow direction matrix, which serves as the central input argument for the calculation of other variables, must then be derived from the hydrologically conditioned DEM. Among the several flow routing algorithms available (e.g. the multiple flow direction algorithm, MD8 by Quinn, Beven, Chevallier, & Planchon, 1991; Tarboton's (1997) D∞ approach; the triangular multiple flow direction algorithm (MD∞) by Seibert & McGlynn, 2007) performing differently in reconstructing the hydrologic pathway, we adopted the flow direction derived from the single-direction flow algorithm, D8 (O'Callaghan & Mark, 1984). It is the most widely used algorithm to delineate drainage networks and catchments from a DEM due to its simplicity, the provision of a reasonable representation for convergent flow conditions, and reduced execution time.

Subsequently, the flow accumulation can be obtained, which leads to the estimation of the upslope contributing area. In order to have flow accumulation values coherent with the actual portions of the surface draining into a cell, it is essential that the analyses are performed on a portion of earth surface confined by a drainage divide (a hydrographic basin) and not by administrative boundaries. Many GIS software applications, QGIS included, contain routines to perform these kinds of hydrologic analyses.

3.1.3. Calibration

The GFA tool performs a terrain analysis using the specified raster grid, and calculates several variables for each basin location (each grid cell): i) local slope, G; ii) drainage network; iii) hydrological paths; iv) difference in elevation between that location and the closest point of the drainage network (H); and v) upslope contributing area in the closest point of the drainage network (A_r). These outputs are also raster grid and are functional to the estimation of the GFI, whose values are then normalized in the range -1:1.

The GFI is transformed into a binary map of flood-prone areas applying a threshold value τ. This parameter is calibrated iteratively, generating binary maps of potential flood-prone areas that are compared with the flood map assumed as reference standard data.

From the comparison, the following performances are assessed: rates of true positives (TP), false positives (FP), true negatives (TN), and false negatives (FN) (e.g. Clubb et al., 2017; Manfreda, Nardi, et al., 2014; Manfreda, Samela, et al., 2014; Orlandini, Tarolli, Moretti, & Dalla Fontana, 2011; Samela, Manfreda, et al., 2017; Samela, Troy,

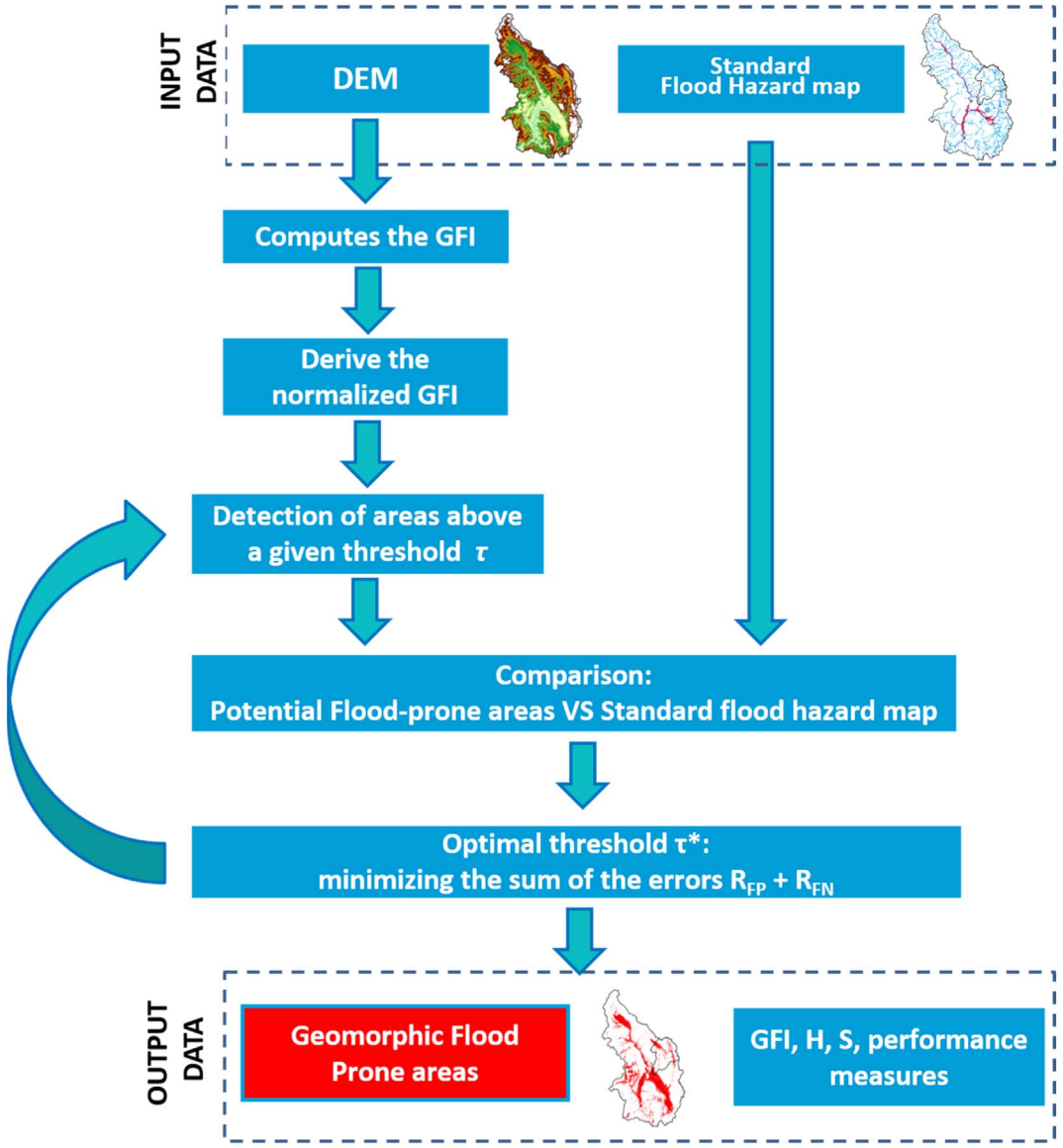

Fig. 1. Schematic description of the algorithm implemented within the GFA tool.

et al., 2017).

The value of τ which minimizes the sum of overestimation (R_{FP}, false positive rate) and underestimation error (R_{FN}, false negative rate), assigning equal weights to the two errors, is taken as the as optimal to distinguish between flood-prone areas and areas not prone to floods for the investigated basin. That calibrated threshold is then applied to the GFI map of the undetermined areas of the whole basin to finally identify the geomorphic flood-susceptible areas. Fig. 1 provides an overview of the methodology described.

3.2. Potential applications

The proposed DEM-based approach may be used to delineate flood-prone area boundaries in areas where hydrologic and hydraulic studies have not been or cannot be conducted. Usually, unstudied zones are located in rural areas or along small streams and the following situations may occur in a river basin at any spatial scale, as schematized in Fig. 2:

i) the main river stem has been studied but no information is available regarding its tributaries, especially the lowest order streams and minor tributaries;
ii) some sub-catchments (tributaries) have been investigated in a given river basin but others are still unstudied;
iii) the river basin has been mapped almost entirely but there are scattered gaps that may depend on different administrative units.

3.3. GFA tool implementation: libraries and system requirements

The GFA tool is developed using a Python programming language (www.python.org) as a QGIS plugin (www.qgis.org). According to the World Bank (2014), the QGIS represents an innovative open source geospatial tool that is lowering the financial barriers to describe risks at national and sub-national levels. It is considered already reasonably mature (working quality code) and it is supported by a substantial and diverse developer and user community (e.g. Albano, Mancusi, Sole, & Adamowski, 2015; Brovelli, Minghini, Moreno-Sanchez, & Oliveira, 2017; Graser & Olaya, 2015; World Bank, 2014). The GFA tool runs on Linux, OS X, and Microsoft Windows operating systems. It requires QGIS 2 or higher for operation, and was specifically tested on the 2.14 x Essen Long Term Release of QGIS.

The GFA tool works just like standard QGIS processing

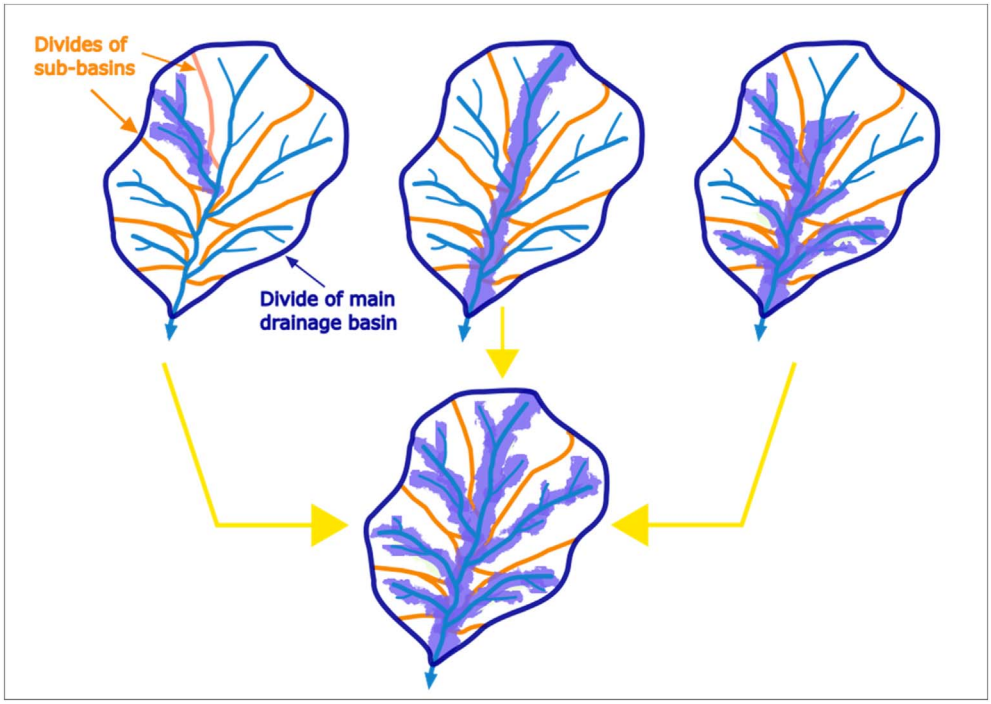

Fig. 2. This image shows how the GFA tool may be used to derive a preliminary, but complete, flood susceptibility map starting from incomplete flood hazard maps.

(geoprocessing) tools and can be accessed from the QGIS user interface. Moreover, thanks to the QGIS plugin architecture, the GFA tool inherits several native advantages of QGIS, e.g. interoperability, portability (available for Windows, Linux, OS and Android), diffusion, modularity and flexibility. This allows easy sharing of tools among users and researchers, and facilitates amendments and addition of improvements and new algorithms (Albano, Mancusi, & Abbate, 2017). The GFA tool already offers a suit of sophisticated analytical capabilities and, because the source code is open and modular, developers can integrate or extract and reuse some of their functionality to incorporate it into larger more complex analytical and simulation systems of both physical and human-environment interactions (Albano, Mancusi, Sole, & Adamowski, 2017). For example, the proposed software can be used as platforms to seamlessly integrate and analyse this diverse information which can be accessed and distributed over a larger web-system in the future.

The GFA tool has taken advantage of the integration of Python with the well-known GDAL (Geospatial Data Abstraction Library) library (www.gdal.org) for manipulation and elaboration of spatial data (e.g. reading and writing raster data, such as DEMs). Furthermore, the GFA tool uses the numeric extension NumPy (www.numpy.org) for scientific computing to include support for powerful N-dimensional array objects. In fact, NumPy allows the efficient manipulation of numerically intensive operation on raster data. Performance measures of the linear binary classifier have been carried out by scikit-learn numeric libraries (www.scikit-learn.org).

3.4. GFA tool components and functionalities

A graphical user interface (GUI) has been designed to simplify the interaction with the end-users, as shown in Fig. 3. The interface is composed of the following boxes.

3.4.1. Input

Four layers are required as input data in the plugin interface: i) DEM; ii) depressionless DEM; iii) flow direction; and iv) flow accumulation. These layers can be selected in the pop-up menus of the tool interface whether calculations are done using QGIS or another software.

3.4.2. Set methodology options

Four options must be specified:

1. Flow direction coding algorithm that has been used to produce the flow direction loaded. A pop-up menu allows users to choose between three possible algorithms: ESRI (Greenlee, 1987; Jenson & Domingue, 1988), HyGRID2k2 (Cazorzi, 2002), TauDEM (Garbrecht & Martz, 1997; Tarboton, 1997).
2. Criterion for drainage network identification contains two possible choices:
   i. the channel starts from locations where the area-slope factor AS^k (where A is the drained area in a point, S is the local slope, and k is a parameter generally set equal to 1.7) is higher than a specific threshold (see Giannoni, Roth, & Rudari, 2005);
   ii. the channel starts from locations where the flow accumulation is higher than a specific threshold.
3. Threshold for the identification of the drainage network in the "Threshold channel" spin control.
4. Hydraulic scaling relation exponent, used for the estimation of the water level (h_r) in each cell of the basin assuming a scaling relationship with the contributing area: $h_r \approx A_r^n$. The power law mentioned, and therefore the exponent n, can be estimated based on hydraulic data obtained from gauging stations located within the investigated basin (see Samela, Troy, et al., 2017), or can be taken from literature (e.g. Engelund & Hansen, 1967; Ibbitt, 1997; Ibbitt, Mckerchar, & Duncan, 1998; Knighton, 2014; Leopold & Maddock, 1953; Leopold, Wolman, & Miller, 1965; Li, 1974; McKerchar, Ibbitt, Brown, & Duncan, 1998; Nardi et al., 2006; Nobre et al., 2011; Park, 1977; Rodriguez-Iturbe & Rinaldo, 1997; Smith, 1974; Whiting, Stamm, Moog, & Orndorff, 1999).

3.4.3. Set calibration options

Here, the user is given the chance to specify the normalized threshold (manually set threshold) which the tool will apply to the GFI map to seek for flood-prone locations. Basin cells that have a value of GFI higher than the imposed threshold will be targeted as flood-prone,

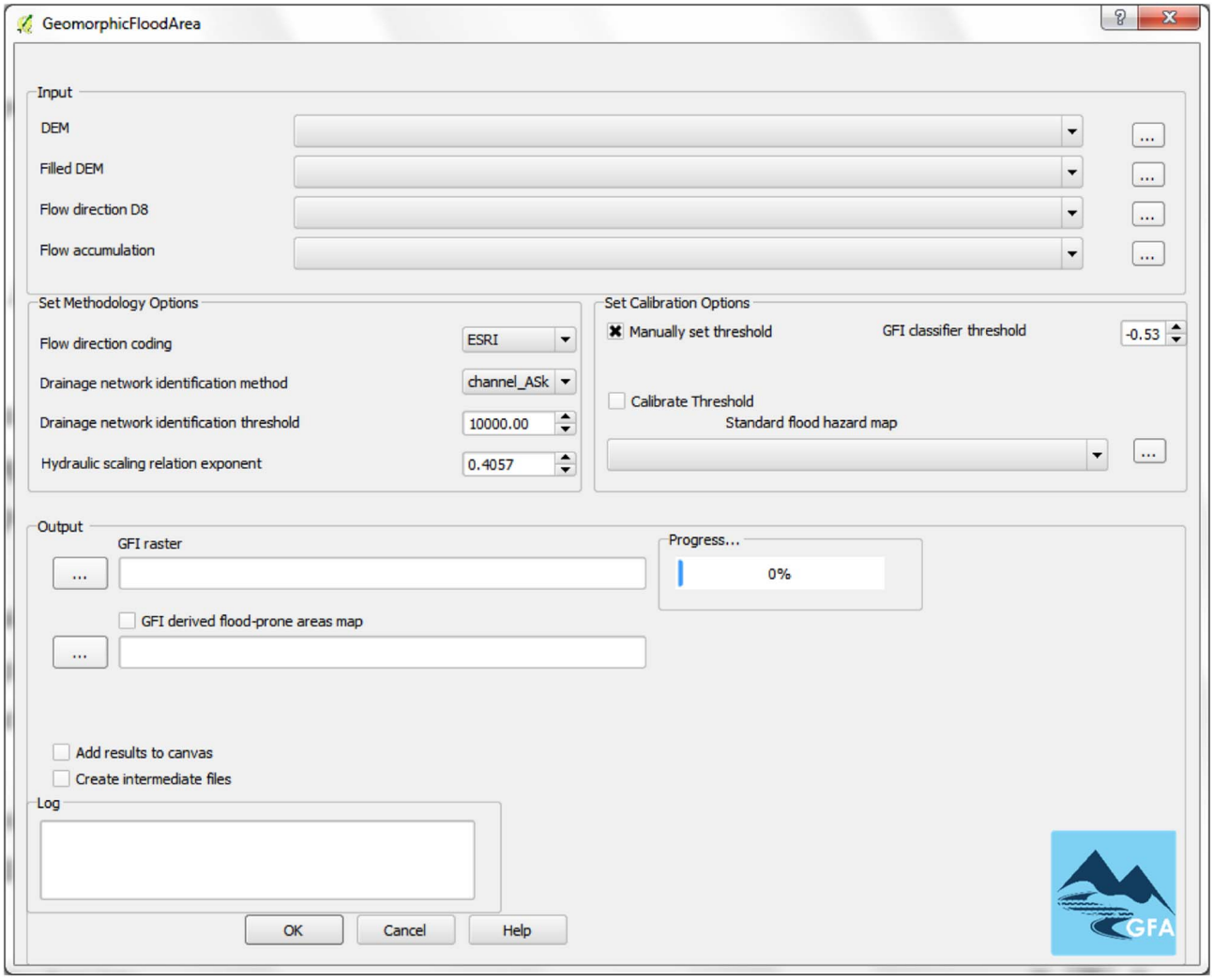

Fig. 3. The Geomorphic Flood Area (GFA) tool window and the GFA tool icon in QGIS.

and conversely. In this case, the chosen threshold must be specified in the "GFI classifier threshold" spin control. Otherwise, users can decide to enable "Calibrate threshold" and, in this case, a standard flood hazard map to use for the scope must be selected.

3.4.4. Output

Given the input data, the tool runs a terrain analysis to compute several intermediate variables for each basin location (each DEM cell). These rasters may be saved in specific files, or exclusively used within the procedure to calculate the GFI. The optimal normalized threshold is calibrated within the training area, and then applied to perform the delineation of the flood-prone areas across the whole investigated basin. In addition to the above-mentioned maps, the code save a *.txt file provides some performance metrics, such as: the calibrated threshold, the false positive rate (R_{FP}), the false negative rate (R_{FN}), the sum $R_{FP} + R_{FN}$, and the Area Under the Curve (AUC) representing the area under the ROC (Receiver Operating Characteristic) curve (0.5 means random classifier and 1 means perfect agreement).

4. GFA tool demonstrative application

A demonstrative application of the GFA tool is presented, illustrating how simplified procedures can help fill the gaps in the maps obtained by hydraulic analyses as well as to give preliminary information on flood hazard exposure in poorly gauged basins and unstudied areas.

4.1. The Romania case study

Romania is an interesting study case, known as one of the most flood-prone countries in Europe. In recent years, Romania has suffered many floods of different types, which have caused huge material damage and many losses of life (Albano, Crăciun, Mancusi, Sole, & Ozunu, 2017; Constantin-Horia, Simona, Gabriela, & Adrian, 2009). For instance, the cyclone that affected a large area of Southeastern and Central Europe in May 2014 produced > 8000 people isolated and nearly 2000 ha of inundated areas in Romania.

The total surface area of Romanian is about 238,000 km^2; 97.8% of it is included in the Danube River Basin (and 30% of the Danube River Basin is in Romania). The geomorphic classification must be applied on a hydrographic basin in order for it to be correctly performed. Hence, to cover the full country, several hydrographic basins, completely or partially contained in the Romanian territory, were selected and the total investigated area was extended outside the national border. Specifically, the country was sub-divided into five major drainage basins, as shown in Fig. 4.

4.2. Application of the GFA tool

To extract the fluvial geomorphology, the SRTM 1 Arc-Second Global elevation data obtained from the USGS was used. It provides worldwide coverage of void filled data at a resolution of 1 arc-second (30 m).

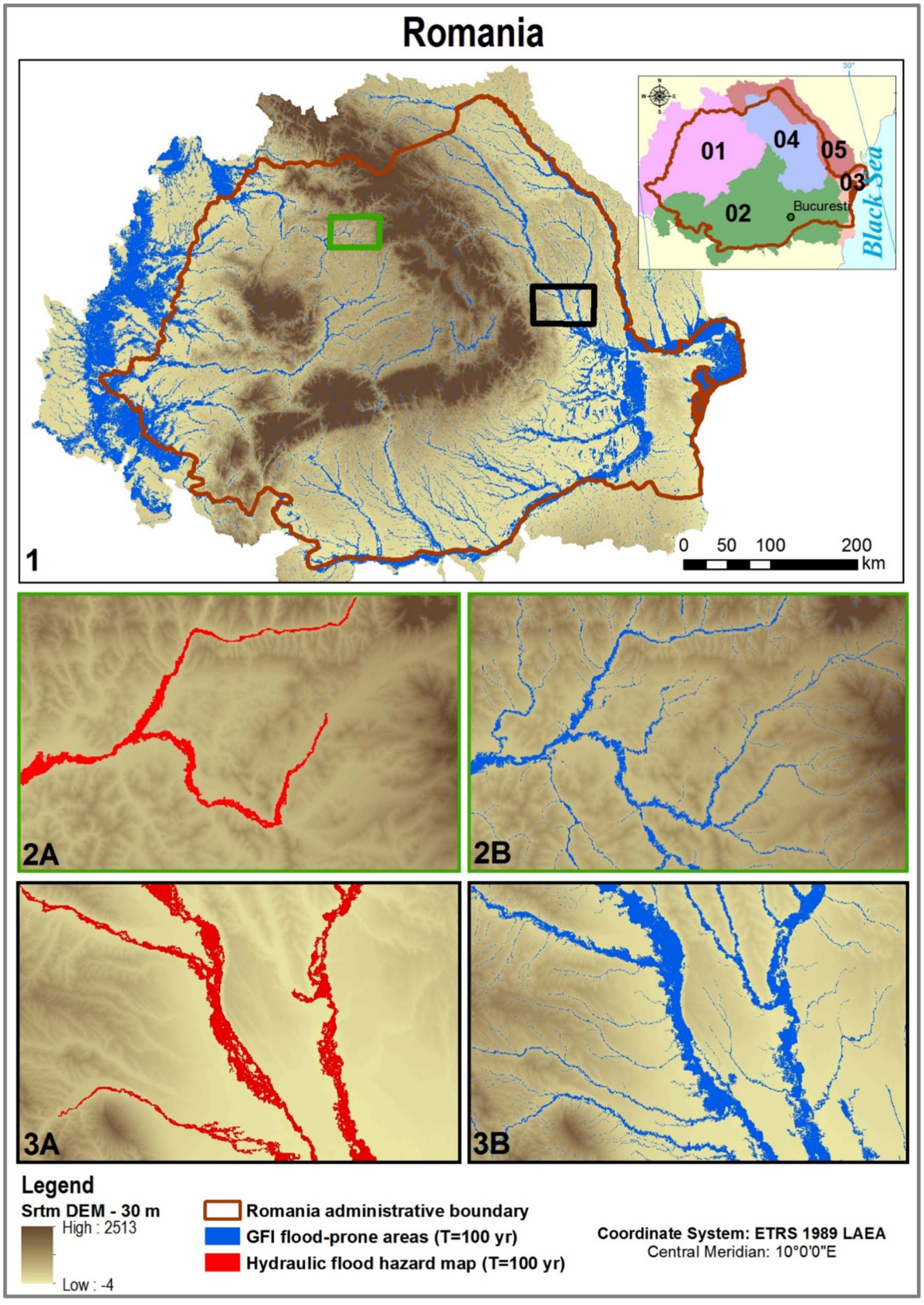

Fig. 4. Panel 1 represents the five major drainage basins identified to study the entire Romania. It also shows the 100-year flood-prone areas identified using the GFA tool (depicted in dark blue). The following two couples of images provide a more detailed comparison between these geomorphic flood-prone areas and the pan-European flood hazard map (Alfieri et al., 2014) used to calibrate the linear binary classification. (For interpretation of the references to colour in this figure legend, the reader is referred to the web version of this article.)

In addition, the pan-European flood hazard map by Alfieri et al. (2014) was adopted as standard map to calibrate the classifier. The map was determined for a return period of 100 years by applying a combination of distributed hydrologic and hydraulic models, and it provides a rough description of flood hazard along the main pan-European rivers with a resolution of 100 m. To carry out the binary

classification, the standard flood hazard map was resampled to a 30-m resolution (the same as the adopted DEM), and converted into a binary map, where the value 1 represents flood-prone areas and the value 0 those not prone to floods (areas of minimal flood hazard). The standard map also contains large areas of undetermined but possible flood hazards that were not used for calibration, and that were filled by the proposed procedure; the training area had an extent larger than 2% in each basin selected. Therefore, the parameter calibration should lead to a reliable threshold value. The value of the exponent n of the hydraulic scaling relationship has been estimated as the average among values found in literature (Engelund & Hansen, 1967; Ibbitt, 1997; Ibbitt et al., 1998; Knighton, 2014; Leopold et al., 1965; Leopold & Maddock, 1953; Li, 1974; McKerchar et al., 1998; Park, 1977; Rodriguez-Iturbe & Rinaldo, 1997; Smith, 1974; Whiting et al., 1999). The mean value estimated is $n = 0.3544$.

The time required to perform the analyses is proportional to the number of cells, independent of their size (pixel resolution). The larger the number of rows and columns of the raster, the greater the time needed to complete the mapping. For example, deriving the flood-prone areas map for basin 4, shown in Fig. 4 (number of rows 1447, number of columns 11,089), required 1567 s (about 26 min). These analyses were carried out using a Dell Precision Workstation T5810, Intel Xeon Processor CPU E5-1620 v3 @ 3.50GHz, 16 GB RAM.

A pictorial representation of the resulting flood-prone areas is reported in Fig. 4. The large-scale map illustrates that the index produces a realistic description of the flood-prone areas, with the possibility to extend the flood hazard information to those portions of the country where the Pan-EU Flood Hazard maps are lacking. Fig. 4 also provides four panels with a comparison of the two flood maps: the training one (red surface) and the GFA output (blue surface). This picture clearly depicts the potential of such procedure, which allowed downscaling of the information contained in the pan-European flood hazard map to the scale of 30 m. It also provided critical information about secondary streams that were not considered in the hydraulic simulation by Alfieri et al. (2014) for computing time limitations.

Table 1 reports quantitative information about the five investigated basins, such as the extent of the training areas adopted (as a percentage of the total basin area), the calibration results in terms of optimal thresholds for the GFI classifier, and the relative performance measures. Correct identification of the areas exposed is always higher than 80% and the classification suffers more from overestimation than underestimation, especially in basin 3, which is a coastal basin where the Danube Delta and the Razim–Sinoe lagoons are located. In these areas, the method is less accurate due to the weak contrast in elevation and slope between the areas exposed to floods and the surrounding landscape. In fact, the Danube Delta is a low alluvial plain, mostly covered by wetlands and water, with 20% of the territory below sea level and more than half not exceeding 1 m in altitude (average altitude is 0.52 m) (Panin, 2003).

The results demonstrate that the linear binary classification may help in designing new strategies for the delineation of flood-prone areas for large-scale applications and in data-scarce environments. It provides good detection accuracies with simple data requirements, low costs and reduced computational time. This kind of simplified approach is generally of great interest to both researchers and decision-makers as increasing portions of populations live in areas affected by flooding in developing countries where data availability is often poor.

5. Conclusion

Flood risk assessment in poor-data environments poses a great challenge that requires the development of new tools and algorithms. In this context, the Geomorphic Flood Index has an extraordinary potential for the mapping of flood-prone areas as has been proven by previous studies (e.g. Manfreda et al., 2015; Samela, Troy, et al., 2017). In order to make such tool available to a larger community, we decided to implement the proposed algorithm in an open-source QGIS plugin named Geomorphic Flood Area tool (GFA tool). It is designed to make the procedure freely available to all users in a user-friendly interface. In this way, anyone can contribute to analyse, modify and redistribute the source code, improving the algorithms and producing new data through a community-based development process that will allow better understanding of the process and increase the production and utilization of pre-elaborated and more understandable data.

We have also presented an application of the tool over a test site. In particular, over the entire territory of Romania (over 238,000 km^2) adopting the SRTM at 30 m of resolution and the Pan-EU flood-hazard map at 100 m of resolution (resampled at 30 m) to generate an extended version of the map, covering the entire territory at a resolution of 30 m. The result is certainly affected by errors and artefacts due to the simplifying assumption of the procedure, but it allows rapid identification of the most exposed areas of the basin without neglecting any stream or reach in the basin. The application testifies to the potential of such QGIS plugin as a flood mapping tool.

The automated identification of floodplains offered by the GFA tool has numerous applications in the geomorphological and hydrological communities and may contribute to overcome current limitations in flood hazard mapping. This approach may be particularly helpful for preliminary flood hazard and risk assessment over large areas and in trans-boundary regions. It may be used by a large community that has been invited to exchange data and experiences with our research group (HydroLAB). In fact, the main aim of such a study is the development of a tool that would help global flood hazard mapping, using the knowledge contained in the available flood studies. With this specific aim, our research group is currently developing a web platform that will promote global collaborative and co-operative geomorphic flood mapping of the entire globe.

Availability

The GFA tool executable code and documentation is in the public domain. It may be used, copied, distributed, or redistributed freely. The plugin described by this document can be downloaded for free from the QGIS plugin repository and from the website (https://github.com/HydroLAB-UNIBAS/GFA-Geomorphic-Flood-Area).

Acknowledgements

This work was carried out within a scientific agreement between the Civil Protection Department of Basilicata, the Interuniversity

Table 1
Values of the optimal thresholds and relative performance measures obtained in calibrating the classifier over the investigated basins.

Basin number	% training area	τ	R_{TP}	R_{FN}	R_{TN}	R_{FP}	Obj. function = R_{FN} + R_{FP}	AUC
1	14%	−0.23	81.9%	18.1%	64.6%	35.4%	53.4%	0.81
2	12%	−0.24	85.0%	15.0%	83.3%	16.7%	31.7%	0.92
3	14%	−0.12	90.6%	9.4%	36.9%	63.1%	72.5%	0.63
4	6%	−0.26	82.6%	17.4%	84.0%	16.0%	33.4%	0.92
5	5%	−0.31	91.1%	8.9%	91.7%	8.3%	17.2%	0.97

Consortium for Hydrology (CINID), and the University of Basilicata to the start-up the Basilicata Hydrologic Risk Center. Authors would like to express their gratitude to the anonymous reviewers for their constructive comments and suggestions that helped to improve the manuscript.

References

Albano, R., Crăciun, I., Mancusi, L., Sole, A., & Ozunu, A. (2017). Flood damage assessment and uncertainty analysis: The case study of 2006 flood in Ilisua basin in Romania. *Carpathian Journal of Earth and Environmental Sciences, 12*.

Albano, R., Mancusi, L., & Abbate, A. (2017). Improving flood risk analysis for effectively supporting the implementation of flood risk management plans: The case study of "Serio" Valley. *Environmental Science & Policy, 75*, 158–172. http://dx.doi.org/10.1016/j.envsci.2017.05.017.

Albano, R., Mancusi, L., Sole, A., & Adamowski, J. (2015). Collaborative strategies for sustainable EU flood risk management: FOSS and geospatial tools—Challenges and opportunities for operative risk analysis. *ISPRS International Journal of Geo-Information, 4*, 2704–2727. http://dx.doi.org/10.3390/ijgi4042704.

Albano, R., Mancusi, L., Sole, A., & Adamowski, J. (2017). FloodRisk: A collaborative, free and open-source software for flood risk analysis. *Geomatics, Natural Hazards and Risk, 8*, 1812–1832. http://dx.doi.org/10.1080/19475705.2017.1388854.

Alfieri, L., Salamon, P., Bianchi, A., Neal, J., Bates, P., & Feyen, L. (2014). Advances in pan-European flood hazard mapping. *Hydrological Processes, 28*, 4067–4077. http://dx.doi.org/10.1002/hyp.9947.

Arnaud-Fassetta, G., Astrade, L., Bardou, É., Corbonnois, J., Delahaye, D., Fort, M., ... Penven, M.-J. (2009). Fluvial geomorphology and flood-risk management. *Géomorphologie Reli. Process. Environ. 15*, 109–128. http://dx.doi.org/10.4000/geomorphologie.7554.

Beven, K. J., & Kirkby, M. J. (1979). A physically based, variable contributing area model of basin hydrology. *Hydrological Sciences Bulletin, 24*, 43–69. http://dx.doi.org/10.1080/02626667909491834.

Bradley, A. A., Cooper, P. J., Potter, K. W., & Price, T. (1996). Floodplain mapping using continuous hydrologic and hydraulic simulation models. *Journal of Hydrologic Engineering, 1*, 63–68. http://dx.doi.org/10.1061/(asce)1084-0699(1996)1:2(63).

Brovelli, M. A., Minghini, M., Moreno-Sanchez, R., & Oliveira, R. (2017). Free and open source software for geospatial applications (FOSS4G) to support Future Earth. *International Journal of Digital Earth, 10*, 386–404. http://dx.doi.org/10.1080/17538947.2016.1196505.

Cazorzi, F. (2002). *Software GIS HydroGrid2002 (HyGrid2k2)*.

Clubb, F. J., Mudd, S. M., Milodowski, D. T., Valters, D. A., Slater, L. J., Hurst, M. D., & Limaye, A. B. (2017). Geomorphometric delineation of floodplains and terraces from objectively defined topographic thresholds. *Earth Surface Dynamics, 5*, 369–385. http://dx.doi.org/10.5194/esurf-5-369-2017.

Constantin-Horia, B., Simona, S., Gabriela, P., & Adrian, S. (2009). Human factors in the floods of Romania. In J. A. A. Jones, T. G. Vardanian, & C. Hakopian (Eds.). *Threats to global water security* (pp. 187–192). Dordrecht: Springer. http://dx.doi.org/10.1007/978-90-481-2344-5_20.

D'Addabbo, A., Refice, A., Pasquariello, G., Lovergine, F. P., Capolongo, D., & Manfreda, S. (2016). A Bayesian network for flood detection combining SAR imagery and ancillary data. *IEEE Transactions on Geoscience and Remote Sensing, 54*, 3612–3625. http://dx.doi.org/10.1109/TGRS.2016.2520487.

De Risi, R., Jalayer, F., & De Paola, F. (2015). Meso-scale hazard zoning of potentially flood prone areas. *Journal of Hydrology, 527*, 316–325. http://dx.doi.org/10.1016/j.jhydrol.2015.04.070.

Degiorgis, M., Gnecco, G., Gorni, S., Roth, G., Sanguineti, M., & Taramasso, A. C. (2012). Classifiers for the detection of flood-prone areas using remote sensed elevation data. *Journal of Hydrology, 470–471*, 302–315. http://dx.doi.org/10.1016/j.jhydrol.2012.09.006.

Degiorgis, M., Gnecco, G., Gorni, S., Roth, G., Sanguineti, M., & Taramasso, A. C. (2013). Flood hazard assessment via threshold binary classifiers: Case study of the tanaro river basin. *Irrigation and Drainage, 62*, 1–10. http://dx.doi.org/10.1002/ird.1806.

Di Baldassarre, G., Schumann, G., & Bates, P. (2009). Near real time satellite imagery to support and verify timely flood modelling. *Hydrological Processes, 23*, 799–803. http://dx.doi.org/10.1002/hyp.7229.

Di Leo, M., Manfreda, S., & Fiorentino, M. (2011). An automated procedure for the detection of flood prone areas: r.hazard.flood. *Geomatics Work, 10*, 1689–1699. http://dx.doi.org/10.1017/CBO9781107415324.004.

Dodov, B.a., & Foufoula-Georgiou, E. (2006). Floodplain morphometry extraction from a high-resolution digital elevation model: A simple algorithm for regional analysis studies. *IEEE Geoscience and Remote Sensing Letters, 3*, 410–413. http://dx.doi.org/10.1109/LGRS.2006.874161.

Engelund, F., & Hansen, E. (1967). A monograph on sediment transport in alluvial streams. *Monografia, 65*. http://dx.doi.org/10.1007/s13398-014-0173-7.2.

FEMA (Federal Emergency Management Agency) (2006). *Floodplain Management Requirements: A Study Guide and Desk Reference for Local Officials*.

Gallant, J. C., & Dowling, T. I. (2003). A multiresolution index of valley bottom flatness for mapping depositional areas. *Water Resources Research, 39*. http://dx.doi.org/10.1029/2002WR001426.

Garbrecht, J., & Martz, L. A. (1997). The assignment of drainage direction over flat surfaces in raster DEM. *Journal of Hydrology,* 204–213. http://dx.doi.org/10.1016/S0022-1694(96)03138-1.

Giannoni, F., Roth, G., & Rudari, R. (2005). A procedure for drainage network identification from geomorphology and its application to the prediction of the hydrologic response. *Advances in Water Resources, 28*, 567–581. http://dx.doi.org/10.1016/j.advwatres.2004.11.013.

Graser, A., & Olaya, V. (2015). Processing: A python framework for the seamless integration of geoprocessing tools in QGIS. *ISPRS International Journal of Geo-Information, 4*, 2219–2245. http://dx.doi.org/10.3390/ijgi4042219.

Greenlee, D. D. (1987). Raster and vector processing for scanned linework. *Photogrammetric Engineering and Remote Sensing, 53*, 1383–1387.

Grimaldi, S., Nardi, F., Di Benedetto, F., Istanbulluoglu, E., & Bras, R. L. (2007). A physically-based method for removing pits in digital elevation models. *Advances in Water Resources, 30*, 2151–2158. http://dx.doi.org/10.1016/j.advwatres.2006.11.016.

Ibbitt, R. P. (1997). Evaluation of optimal channel network and river basin heterogeneity concepts using measured flow and channel properties. *Journal of Hydrology, 196*, 119–138. http://dx.doi.org/10.1016/S0022-1694(96)03293-3.

Ibbitt, R. P., Mckerchar, A. I., & Duncan, M. J. (1998). Taieri River data to test channel network and river basin heterogeneity concepts. *Water Resources Research, 34*, 2085–2088. http://dx.doi.org/10.1029/98WR00483.

Jafarzadegan, K., & Merwade, V. (2017). A DEM-based approach for large-scale floodplain mapping in ungauged watersheds. *Journal of Hydrology, 550*, 650–662. http://dx.doi.org/10.1016/j.jhydrol.2017.04.053.

Jenson, S. K., & Domingue, J. O. (1988). Extracting topographic structure from digital elevation data for geographic information system analysis. *Photogrammetric Engineering and Remote Sensing, 54*, 1593–1600 (https://doi.org/0099-1112/88/5411-1593$02.25/0).

Jonkman, S. N. (2005). Global perspectives on loss of human life caused by floods. *Natural Hazards, 34*, 151–175. http://dx.doi.org/10.1007/s11069-004-8891-3.

Kenward, T. (2000). Effects of digital elevation model accuracy on hydrologic predictions. *Remote Sensing of Environment, 74*, 432–444. http://dx.doi.org/10.1016/S0034-4257(00)00136-X.

Knebl, M. R., Yang, Z. L., Hutchison, K., & Maidment, D. R. (2005). Regional scale flood modeling using NEXRAD rainfall, GIS, and HEC-HMS/RAS: A case study for the San Antonio River Basin Summer 2002 storm event. *Journal of Environmental Management, 75*, 325–336. http://dx.doi.org/10.1016/j.jenvman.2004.11.024.

Knighton, D. (2014). *Fluvial forms and processes: A new perspective*.

Leopold, L. B., & Maddock, T. J. (1953). The hydraulic geometry of stream channels and some physiographic implications. *Geological survey professional paper 252*http://dx.doi.org/10.1016/S0169-555X(96)00028-1.

Leopold, L. B., Wolman, M. G., & Miller, J. P. (1965). Fluvial processes in geomorphology. *Journal of Hydrology*. http://dx.doi.org/10.1016/0022-1694(65)90101-0.

Li, R. (1974). *Mathematical modeling of response from small watershed*.

Lindsay, J. B., & Creed, I. F. (2005). Removal of artifact depressions from digital elevation models: Towards a minimum impact approach. *Hydrological Processes, 19*, 3113–3126. http://dx.doi.org/10.1002/hyp.5835.

Manfreda, S., Di Leo, M., & Sole, A. (2011). Detection of flood-prone areas using digital elevation models. *Journal of Hydrologic Engineering, 16*, 781–790. http://dx.doi.org/10.1061/(ASCE)HE.1943-5584.0000367.

Manfreda, S., Nardi, F., Samela, C., Grimaldi, S., Taramasso, A. C., Roth, G., & Sole, A. (2014). Investigation on the use of geomorphic approaches for the delineation of flood prone areas. *Journal of Hydrology, 517*. http://dx.doi.org/10.1016/j.jhydrol.2014.06.009.

Manfreda, S., Samela, C., Gioia, A., Consoli, G., Iacobellis, V., Giuzio, L., Cantisani, A., & Sole, A. (2015). Flood-prone areas assessment using linear binary classifiers based on flood maps obtained from 1D and 2D hydraulic models. *Natural Hazards, 79*. http://dx.doi.org/10.1007/s11069-015-1869-5.

Manfreda, S., Samela, C., Sole, A., & Fiorentino, M. (2014). Flood-prone areas assessment using linear binary classifiers based on morphological indices. *Vulnerability, uncertainty, risk* (pp. 2002–2011). . http://dx.doi.org/10.1061/9780784413609.201.

Martz, L. W., & Garbrecht, J. (1998). The treatment of flat areas and depressions in automated drainage analysis of raster digital elevation models. *Hydrological Processes, 12*, 843–855. http://dx.doi.org/10.1002/(SICI)1099-1085(199805)12:6<843::AID-HYP658>3.0.CO;2-R.

Martz, L. W., & Garbrecht, J. (1999). An outlet breaching algorithm for the treatment of closed depressions in a raster DEM. *Computational Geosciences, 25*, 835–844. http://dx.doi.org/10.1016/S0098-3004(99)00018-7.

McGlynn, B. L., & Seibert, J. (2003). Distributed assessment of contributing area and riparian buffering along stream networks. *Water Resources Research, 39*. http://dx.doi.org/10.1029/2002WR001521.

McKerchar, A. I., Ibbitt, R. P., Brown, S. L. R., & Duncan, M. J. (1998). Data for Ashley River to test channel network and river basin heterogeneity concepts. *Water Resources Research, 34*, 139–142. http://dx.doi.org/10.1029/98WR00483.

Munich, R. E. (2005). Topics Geo, annual review, natural catastrophes 2005. *Knowledge series*Munich, Germany: Topics Geo (2006, https://doi.org/Yes).

Nardi, F., Biscarini, C., Di Francesco, S., Manciola, P., & Ubertini, L. (2013). Comparing a large-scale dem-based floodplain delineation algorithm with standard flood maps: The tiber river basin case study. *Irrigation and Drainage, 62*, 11–19. http://dx.doi.org/10.1002/ird.1818.

Nardi, F., Grimaldi, S., Santini, M., Petroselli, A., & Ubertini, L. (2008). Hydrogeomorphic properties of simulated drainage patterns using digital elevation models: The flat area issue. *Hydrological Sciences Journal, 53*, 1176–1193. http://dx.doi.org/10.1623/hysj.53.6.1176.

Nardi, F., Vivoni, E. R., & Grimaldi, S. (2006). Investigating a floodplain scaling relation using a hydrogeomorphic delineation method. *Water Resources Research, 42*. http://dx.doi.org/10.1029/2005WR004155.

Nobre, A. D., Cuartas, L. A., Hodnett, M., Rennó, C. D., Rodrigues, G., Silveira, A., ... Saleska, S. (2011). Height Above the Nearest Drainage - A hydrologically relevant new terrain model. *Journal of Hydrology, 404*, 13–29. http://dx.doi.org/10.1016/j.

jhydrol.2011.03.051.

Noman, N. S., Nelson, E. J., & Zundel, A. K. (2001). Review of automated floodplain delineation from digital terrain models. *Journal of Water Resources Planning and Management, 127*, 394–402. http://dx.doi.org/10.1061/(ASCE)0733-9496(2001)127:6(394).

O'Callaghan, J. F., & Mark, D. M. (1984). The extraction of drainage networks from digital elevation data. *Computer Vision, Graphics, and Image Processing, 27*, 247. http://dx.doi.org/10.1016/S0734-189X(84)80047-X.

Olivera, F., Famiglietti, J., & Asante, K. (2000). Global-scale flow routing using a source-to-sink algorithm. *Water Resources Research, 36*, 2197–2207. http://dx.doi.org/10.1029/2000WR900113.

Orlandini, S., Tarolli, P., Moretti, G., & Dalla Fontana, G. (2011). On the prediction of channel heads in a complex alpine terrain using gridded elevation data. *Water Resources Research, 47*(2), W02538. http://dx.doi.org/10.1029/2010WR009648.

Panin, N. (2003). The Danube Delta. Geomorphology and Holocene Evolution: a synthesis/Le delta du Danube. Géomorphologie et évolution holocène: une synthèse. *Géomorphologie: relief, processus, environnement, Octobre-décembre, 9*(4), 247–262. http://dx.doi.org/10.3406/morfo.2003.1188.

Park, C. C. (1977). World-wide variations in hydraulic geometry exponents of stream channels: An analysis and some observations. *Journal of Hydrology, 33*, 133–146. http://dx.doi.org/10.1016/0022-1694(77)90103-2.

Planchon, O., & Darboux, F. (2002). A fast, simple and versatile algorithm to fill the depressions of digital elevation models. *Catena,* 159–176. http://dx.doi.org/10.1016/S0341-8162(01)00164-3.

Quinn, P., Beven, K., Chevallier, P., & Planchon, O. (1991). The prediction of hillslope flow paths for distributed hydrological modelling using digital terrain models. *Hydrological Processes, 5*, 59–79. http://dx.doi.org/10.1002/hyp.3360050106.

Rodriguez-Iturbe, I., & Rinaldo, A. (1997). Fractal river basins: Chance and self-organization. *Power*. http://dx.doi.org/10.1063/1.882305.

Samela, C., Manfreda, S., De Paola, F., Giugni, M., Sole, A., & Fiorentino, M. (2016). DEM-based approaches for the delineation of flood-prone areas in an ungauged basin in Africa. *Journal of Hydrologic Engineering, 21*, 6015010. http://dx.doi.org/10.1061/(ASCE)HE.1943-5584.0001272.

Samela, C., Manfreda, S., & Troy, T. J. (2017). Dataset of 100-year flood susceptibility maps for the continental U.S. derived with a geomorphic method. *Data in Brief, 12*, 203–207. http://dx.doi.org/10.1016/j.dib.2017.03.044.

Samela, C., Troy, T. J., & Manfreda, S. (2017). Geomorphic classifiers for flood-prone areas delineation for data-scarce environments. *Advances in Water Resources, 102*, 13–28. http://dx.doi.org/10.1016/j.advwatres.2017.01.007.

Sanders, B. F. (2007). Evaluation of on-line DEMs for flood inundation modeling. *Advances in Water Resources, 30*, 1831–1843. http://dx.doi.org/10.1016/j.advwatres.2007.02.005.

Santini, M., Grimaldi, S., Nardi, F., Petroselli, A., & Rulli, M. C. (2009). Pre-processing algorithms and landslide modelling on remotely sensed DEMs. *Geomorphology, 113*, 110–125. http://dx.doi.org/10.1016/j.geomorph.2009.03.023.

Schwanghart, W., & Kuhn, N. J. (2010). TopoToolbox: A set of Matlab functions for topographic analysis. *Environmental Modelling and Software, 25*, 770–781. http://dx.doi.org/10.1016/j.envsoft.2009.12.002.

Seibert, J., & McGlynn, B. L. (2007). A new triangular multiple flow direction algorithm for computing upslope areas from gridded digital elevation models. *Water Resources Research, 43*. http://dx.doi.org/10.1029/2006WR005128.

Smith, T. R. (1974). A derivation of the hydraulic geometry of steady-state channels from conservation principles and sediment transport laws. *Journal of Geology, 82*, 98–104. http://dx.doi.org/10.1086/627939.

Soille, P. (2004). Optimal removal of spurious pits in grid digital elevation models. *Water Resources Research, 40*, 1–9. http://dx.doi.org/10.1029/2004WR003060.

Sole, A., Giosa, L., Albano, R., Cantisani, A., Risk, F., & Hydraulics, N. (2013). The laser scan data as a key element in the hydraulic flood modelling in urban areas. *International archives of the Photogrammetry, Remote Sensing and Spatial Information Sciences - ISPRS archives* (pp. 29–31). .

Tarboton, D. G. (1997). A new method for the determination of flow directions and upslope areas in grid digital elevation models. *Water Resources Research, 33*, 309–319. http://dx.doi.org/10.1029/96WR03137.

Tianqi, A., Takeuchi, K., Ishidaira, H., Yoshitani, J., & Fukami, K. (2003). Development and application of a new algorithm for automated pit removal for grid DEMs. *Hydrological Sciences Journal, 48*, 985–998. http://dx.doi.org/10.1623/hysj.48.6.985.51423.

UNISDR, & CRED (2015). *The human cost of weather-related disasters 1995–2015*. UNISDR Publicationshttp://dx.doi.org/10.1017/CBO9781107415324.004.

Vaze, J., Teng, J., & Spencer, G. (2010). Impact of DEM accuracy and resolution on topographic indices. *Environmental Modelling and Software, 25*, 1086–1098. http://dx.doi.org/10.1016/j.envsoft.2010.03.014.

Wang, L., & Liu, H. (2006). An efficient method for identifying and filling surface depressions in digital elevation models for hydrologic analysis and modelling. *International Journal of Geographical Information Science, 20*, 193–213. http://dx.doi.org/10.1080/13658810500433453.

Whiteaker, T. L., Robayo, O., Maidment, D. R., & Obenour, D. (2006). From a NEXRAD rainfall map to a flood inundation map. *Journal of Hydrologic Engineering, 11*, 37–45. http://dx.doi.org/10.1061/(ASCE)1084-0699(2006)11:1(37).

Whiting, P. J., Stamm, J. F., Moog, D. B., & Orndorff, R. L. (1999). Sediment-transporting flows in headwater streams. *Bulletin Geological Society of America, 111*, 450–466. http://dx.doi.org/10.1130/0016-7606(1999)111<0450:STFIHS>2.3.CO;2.

Wolman, M. G. (1971). Evaluating alternative techniques floodplain mapping. *Water Resources Research, 7*, 1383–1392. http://dx.doi.org/10.1029/WR007i006p01383.

World Bank (2014). *Global Facility for Disaster Reduction and Recovery. Understanding Risk in an Evolving World: Emerging Best Practices in Natural Disaster Risk Assessment. 329*, 1086. http://dx.doi.org/10.1136/bmj.329.7474.1086.

Wu, S., Li, J., & Huang, G. H. (2008). A study on DEM-derived primary topographic attributes for hydrologic applications: Sensitivity to elevation data resolution. *Applied Geography, 28*, 210–223. http://dx.doi.org/10.1016/j.apgeog.2008.02.006.

Yan, K., Di Baldassarre, G., Solomatine, D. P., & Schumann, G. J. P. (2015). A review of low-cost space-borne data for flood modelling: Topography, flood extent and water level. *Hydrological Processes, 29*, 3368–3387. http://dx.doi.org/10.1002/hyp.10449.